BEST AVAILABLE IMAGES

Defective images within this document are accurate representations of the original documents submitted by the applicant.

Defects in the images may include (but are not limited to):

- BLACK BORDERS
- TEXT CUT OFF AT TOP, BOTTOM OR SIDES
- FADED TEXT
- ILLEGIBLE TEXT
- SKEWED/SLANTED IMAGES
- COLORED PHOTOS
- BLACK OR VERY BLACK AND WHITE DARK PHOTOS
- GRAY SCALE DOCUMENTS

IMAGES ARE BEST AVAILABLE COPY.

As rescanning documents *will not* correct images, please do not report the images to the Image Problem Mailbox.

OPIC
OFFICE DE LA PROPRIÉTÉ INTELLECTUELLE DU CANADA

CIPO
CANADIAN INTELLECTUAL PROPERTY OFFICE

(12)(19)(CA) **Demande-Application**

(21)(A1) **2,268,462**
(22) 1999/04/09
(43) 2000/10/09

(72) ROTSTEIN, Ori, CA
(72) JONES, Julia, CA
(71) ROTSTEIN, Ori, CA
(71) JONES, Julia, CA

(51) Int.Cl.[6] A61K 31/22

(54) **METHODE DE PREVENTION DE LA NECROSE ET DE L'APOPTOSE**

(54) **METHOD OF PREVENTING NECROSIS AND APOPTOSIS**

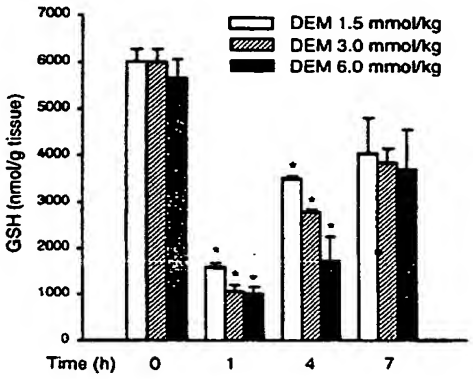

(57) Manipulation of the intracellular redox state has been shown to alter cell activation pathways with resultant changes in cellular function. Previous studies have suggested that thiol oxidation, using the glutathione-depleting agent diethyl maleate, was able to inhibit endothelial cell activation. We hypothesized that this agent might exert beneficial effects following endotoxemia in the rat, a model where transendothelial migration of neutrophils is central to the development of hepatocellular injury. Sprague Dawley rats treated intraperitoneally with LPS (200 µg/kg) plus D-galactosamine (600 mg/kg) developed hepatocellular necrosis, as evidenced by liver enzyme release and morphological changes. Pretreatment with diethyl maleate abrogated this injury in a dose dependent fashion. Histology revealed reduced neutrophil accumulation in both the parenchyma and sinusoids, consistent with reduced neutrophil sequestration and transendothelial migration. This effect appeared to be related to the ability of diethyl maleate to prevent LPS-induced upregulation of both VCAM-1 mRNA and ICAM-1 mRNA in the liver as well as reducing TNF mRNA expression. In addition, diethyl maleate prevented hepatocyte apoptosis followings LPS treatment. The effect was reproduced when TNF was used as an inflammatory stimulus, suggesting a direct protective effect on the hepatocyte. Taken together, these studies show that redox manipulation through thiol oxidation may represent a novel approach to preventing liver necrosis and apoptosis in inflammatory conditions.

ABSTRACT

Manipulation of the intracellular redox state has been shown to alter cell activation pathways with resultant changes in cellular function. Previous studies have suggested that thiol oxidation, using the glutathione-depleting agent diethyl maleate, was able to inhibit endothelial cell activation. We hypothesized that this agent might exert beneficial effects following endotoxemia in the rat, a model where transendothelial migration of neutrophils is central to the development of hepatocellular injury. Sprague Dawley rats treated intraperitoneally with LPS (200 µg/kg) plus D-galactosamine (600 mg/kg) developed hepatocellular necrosis, as evidenced by liver enzyme release and morphological changes. Pretreatment with diethyl maleate abrogated this injury in a dose dependent fashion. Histology revealed reduced neutrophil accumulation in both the parenchyma and sinusoids, consistent with reduced neutrophil sequestration and transendothelial migration. This effect appeared to be related to the ability of diethyl maleate to prevent LPS-induced upregulation of both VCAM-1 mRNA and ICAM-1 mRNA in the liver as well as reducing TNF mRNA expression. In addition, diethyl maleate prevented hepatocyte apoptosis following LPS treatment. The effect was reproduced when TNF was used as an inflammatory stimulus, suggesting a direct protective effect on the hepatocyte . Taken together, these studies show that redox manipulation through thiol oxidation may represent a novel approach to preventing liver necrosis and apoptosis in inflammatory conditions.

Method of Preventing Necrosis and Apoptosis

BACKGROUND OF THE INVENTION

Liver dysfunction is a common complication of systemic infection associated with endotoxemia. Experimental studies have defined a multi-step process which culminates in the development of hepatocellular necrosis following systemic LPS administration (1,2). This is characterized by early sequestration of neutrophils (PMNs) within the hepatic sinusoids, subsequent transmigration of PMNs into the parenchyma and finally interaction of PMNs with parenchymal cells resulting in hepatocellular necrosis. The initial phase of sinusoidal PMN accumulation appears to be independent of well-defined PMN-endothelial cell interactions (3-5). Thus, while adhesion molecules on both cell types are upregulated during endotoxemia, inhibitor studies using antibodies directed against these surface molecules fail to prevent neutrophil sequestration. By contrast, PMN and endothelial cell adhesion molecules appear to be integral to transmigration of PMNs into the hepatic parenchyma and possibly to the subsequent hepatocyte injury (6). For example, treatment with antibodies directed against either ICAM-1 or VCAM-1, both expressed on sinusoidal endothelial cells during endotoxemia, prevent neutrophil infiltration into the liver parenchyma and the consequent enzyme rise associated with widespread parenchymal necrosis (3,4). The important role of TNF in this process is underscored by the failure of endotoxin to induce ICAM-1 expression and hepatocellular injury in endotoxin-resistant animals, while treatment with TNF reproduces these pathological processes (3). A recent report by Jaeschke and colleagues further demonstrated that TNF-induced hepatic parenchymal apoptosis may provide an important signal for PMN transmigration out of the sinusoids into the parenchymal tissues with consequent cellular necrosis (7).

SUMMARY OF THE INVENTION

The invention includes a method of decreasing cell apoptosis and/or cell necrosis in a mammal, comprising administering an effective amount of a glutathione

depleting agent or a pharmaceutically acceptable salt thereof. In one variation, the glutathione depleting agent is selected from the group consisting of diethylmaleate (DEM), a mimetic of DEM having glutathione depleting activity, phorone, a mimetic of phorone having glutathione depleting activity, buthionine sulfoximine (BSO), a mimetic of buthionine sulfoximine (BSO) having glutathione depleting activity and their equivalents. The cell is preferably a hepatocyte, a leukocyte, an endothelial cell or an epithelial cell. Cell apoptosis may be caused by TNF or an apoptosis inducing agent. The cell apoptosis and/or cell necrosis may occur as a result of inflammation, neoplasis, or inherent pre-programmed cell death. The route of administration of the agent is preferably selected from a group consisting of oral administration, aerosol administration, parenteral administration, cavity administration, rectal administration and air passage administration.

The invention includes the use of a glutathione depleting agent or a pharmaceutically acceptable salt thereof in the manufacture of a medicament for decreasing cell apoptosis and/or cell necrosis. The invention also includes the use of a glutathione depleting agent or a pharmaceutically acceptable salt thereof for decreasing cell apoptosis and/or cell necrosis. The glutathione depleting agent is preferably selected from the group consisting of diethylmaleate (DEM), a mimetic of DEM having glutathione depleting activity, phorone, a mimetic of phorone having glutathione depleting activity, buthionine sulfoximine (BSO), a mimetic of buthionine sulfoximine (BSO) having glutathione depleting activity and their equivalents. The cell may be a hepatocyte, a leukocyte, an endothelial cell or an epithelial cell. Cell apoptosis may be caused by TNF or an apoptosis inducing agent. Cell apotosis/or cell necrosis may occur as a result of inflammation, neoplasis, or inherent pre-programmed cell death. The route of administration of the agent is preferably selected from a group consisting of oral administration, aerosol administration, parenteral administration, cavity administration, rectal administration, air passage administration.

Another aspect of the invention relates to a cell apoptosis and/or cell necrosis decreasing pharmaceutical composition, comprising a glutathione depleting agent or a pharmaceutically acceptable salt thereof, in association with a pharmaceutically acceptable carrier. In the composition, preferably the glutathione depleting agent is selected from the group consisting of diethylmaleate (DEM), a mimetic of DEM having

glutathione depleting activity, phorone, a mimetic of phorone having glutathione depleting activity, buthionine sulfoximine (BSO), a mimetic of buthionine sulfoximine (BSO) having glutathione depleting activity and their equivalents. The invention also includes a pharmaceutical package, needle, kit or aerosol delivery device including the composition. The invention includes a method of decreasing cell apoptosis and/or cell necrosis in a mammal, comprising administering an effective amount of the composition. The invention includes the use of the composition in the manufacture of a medicament for decreasing cell apoptosis. Another apsect of the invention includes use of the composition for decreasing cell apoptosis and/or cell necrosis. The invention also includes the composition, package, needle, kit or device for use in decreasing cell apoptosis and/or cell necrosis.

DETAILED DESCRIPTION OF THE INVENTION

The intracellular redox state regulates several aspects of cell function, suggesting that strategies directed toward altering the cellular redox state may modulate cell activation in inflammatory states (8-11). Our previous studies evaluated the effect of diethyl maleate (DEM), an agent which rapidly depletes the most abundant intracellular thiol glutathione, on the ability of LPS to induce endothelial cell activation (12). *In vitro* studies demonstrated that DEM inhibited upregulation of ICAM-1 in response to LPS and prevented PMN transendothelial migration. Lung ICAM-1 expression following intratracheal LPS was similarly inhibited (12). Based on these findings and the central role of endothelial cell adhesion molecule expression in the pathogenesis of endotoxin-induced liver injury, we hypothesized that redox manipulation, through the use of the thiol oxidizing agent DEM, might exert a protective effect on hepatocellular necrosis in a LPS/D-galactosamine rodent model. The present studies show that DEM prevents the LPS/D-galactosamine-induced rise in serum liver enzymes as well as the histological development of parenchymal necrosis. Consistent with our hypothesis, upregulation of

both ICAM-1 and VCAM-1 in the liver was inhibited. Interestingly, DEM prevented both hepatocyte necrosis and apoptosis in this model, even when TNF was used instead of LPS as the inflammatory stimulus. This suggests that DEM might have direct effects on hepatocyte function in addition to its previously reported effects on endothelial cell activation.

MATERIALS AND METHODS

Reagents. *Escherichia coli* 026:B6 lipopolysaccharide (LPS), D (+) galactosamine (GalN), diethyl maleate (DEM), phorone were purchased from Sigma Chemical Company (St. Louis, Mo). FITC-conjugated mouse anti-rat CD11b monoclonal antibody and FITC-conjugated mouse IgG_{2a} isotypic negative control were obtained from Serotec (Toronto, Ontario). The murine ICAM-1 cDNA probe, murine VCAM-1 cDNA probe and murine TNF-α cDNA probes were purchased from American Type Culture Collection.

Induction of Acute Liver Injury. Male Sprague Dawley rats weighing 250-300 g were purchased from Charles River Laboratories (Constante, Quebec). All animal studies were performed in accordance with guidelines set forth by the Toronto Hospital Animal Care Committee and The Canadian Council on Animal Care. Animals were housed in standard clear plastic cages, fed standard rat chow and water ad libitum. The animals were allowed to acclimatize before experiments were started. Liver injury was induced by intraperitoneal injection (i.p.) of 600 mg/kg D-(+) galactosamine (GalN) and 200 µg/kg LPS. Sham animals received an equal volume of sterile normal saline i.p. Glutathione depletion was induced by i.p. injection of DEM (3 mmol/kg) or phorone (250 mg/kg) at various times relative to LPS challenge.

Assessment of Liver Injury. The animals were sacrificed at various intervals over a six hour time course. At the end of the experimental protocol, approximately 3 ml of blood were withdrawn by cardiac puncture into heparinized syringes for evaluation of plasma aspartate aminotransferase (AST). Liver tissue was harvested and snap frozen in liquid nitrogen for evaluation of myeloperoxidase levels, mRNA levels , or NF-κB translocation.

Histologic Evaluation. For standard histologic evaluation, liver tissue was fixed with 10% buffered formalin. Samples were paraffin embedded and cut sections (4 μm) and stained with hematoxylin and eosin stain. Samples were evaluated under light microscopy. Histological sections were also evaluated for apoptosis using in situ end-labeling (13). Sections were evaluated in a blind fashion by an independent observer.

Myeloperoxidase Activity (MPO). Liver tissue (2 g) was homogenized in 4 ml ice cold phosphate buffered saline (20 mmol/L $KHPO_4$, pH 7.4, one min). Following centrifugation (12 000 g, 20 min, 4°C) the supernatant was discarded and the pellet was homogenized again in an equivalent volume of 50 mmol/L phosphate-buffered saline (pH 6.0) containing 0.5% hexadecyltrimethylammonium bromide. This suspension was frozen overnight at -70°C, homogenized (1 min) and sonicated at 40W (1 min). After centrifugation, the supernatant was collected. The protein content of the samples was determined using the Pierce BCA Protein Assay (Pierce, Rockford, IL). MPO activity was assessed as the change in absorbance using a Cobas FARA II Chemistry System (Roche Diagnostic Systems, NJ) at A_{655nm} over three minutes after the addition of 25 μlof 3.0 mM H_2O_2 as previously described (14).

Glutathione Assay. Quantitation of total liver non-protein sulfhydryls (NPSH) was assessed using a DTNB based assay as described by Jocelyn (15). Liver tissue

was thawed, weighed and approximately 0.25 g was homogenized. The resulting acid thiol extract was assayed for NPSH by quantitating the reduction of DTNB through its conversion to 5-thio-2-nitrobenzoic acid at 412 nm using a spectrophotometer. Sample values were then calculated from a standard curve generated using known amounts of reduced glutathione (GSH) and are expressed as GSH equivalents per gram of tissue.

Neutrophil CD11b expression. Neutrophil CD11b receptor expression on whole blood PMNs was assessed as previously described (16). In brief, 100 µl of whole blood was mixed with 10 µl FITC-conjugated mouse anti-rat CD11b monoclonal antibody (Serotec, Toronto, Ontario) or 10 µl of FITC conjugated murine IgG_{2a} isotypic negative control monoclonal antibody (Serotec, Toronto, Ontario) and incubated for 15 min at 25 °C. Red blood cells were lysed with 1 ml of E-lyse and washed with phosphate buffered saline (PBS). PMN CD11b receptor expression was analyzed on a Coulter EPICS XL-MCL flow cytometer (Coutler Co., Hialeah, FL).

RNA extraction and Northern blot analysis. Total RNA was extracted using the guanidium-isothiocyanate method (17). Briefly, liver tissue was harvested from treated animals and immediately frozen in liquid nitrogen. Approximately 100 mg of liver tissue was then thawed and homogenized in 10 ml of 4 M guanidine-isothiocyanate containing 25 mM sodium citrate, 0.5% sarcosyl, and 100 mM β-mercaptoethanol. Messenger RNA was isolated using a messenger RNA extraction kit (Quik Prep Mico Purification Kit, Amersham Pharmacia Biotech, Inc., Baie d'Urfe, Quebec). RNA was denatured, electrophoresed through a 1.2% formaldehyde-agarose gel and transferred to nylon membrane. Hybridization was carried out using a ^{32}P-labeled, random-primed murine ICAM-1 cDNA probe, murine VCAM-1 cDNA probe or murine TNF-α cDNA probe. The mRNA expression was quantitated using a phosphoimager and

accompanying ImageQuant software (Molecular Dynamics, Sunnyvale, CA) and was standardized to G3PDH house keeping gene signal to correct for any variability in gel loading.

Electrophoretic Mobility Shift Assay (EMSA). Nuclear protein extracts were prepared from liver tissue by the method of Deryckere and Gannon (18). Aliquots of 200 - 500 mg of frozen tissue were ground to powder with a mortar in liquid nitrogen. The thawed powder was homogenized in a Dounce tissue homogenizer with 4 ml of solution A (0.6% Nonidet P-40, 150 mM NaCl, 10 mM HEPES, pH 7.9, 1 mM EDTA, and 0.5 mM PMSF). The cells were lysed with five strokes of the pestle. After transfer to a 15-ml tube, debris was pelleted by briefly centrifuging at 2000 rpm for 30 sec. The supernatant was transferred to 50-ml Corex tubes, incubated on ice for 5 min, and centrifuged for 10 min at 5000 rpm. Nuclear pellets were then resuspended in 300 µl of solution B (25% glycerol, 20 mM HEPES, pH 7.9, 420 mM NaCl, 1.2 mM MgCl2, 0.2 mM EDTA, 0.5 mM DTT, 0.5 mM PMSF, 2 mM benzamidine, 5 µg/ml pepstatin, 5 µg/ml leupeptin, and 5 µg/ml aprotinin) and incubated on ice for 20 min. The mixture was transferred to microcentrifuge tubes, and nuclei were pelleted by centrifugation at 14,000 rpm for 1 min. Supernatants containing nuclear proteins were aliquoted in small fractions, frozen in liquid nitrogen and stored at -70°C. Protein quantitation was performed using the BIO-RAD protein assay dye reagent (BIO-RAD, Hercules, CA).

The probe used for EMSA is a 25-bp double-stranded construct (5'-TAGCTT GGAAATTCCGGAGCTGAAG-3') corresponding to a sequence in the ICAM-1 variant NF-κB site (19). End labeling was performed by T4 kinase in the presence of [^{32}P]ATP. Labeled oligonucleotides were purified on a Sephadex G-50 M column (Pharmacia Biotech, Inc., Piscataway, NJ). An aliquot of 5 µg of nuclear protein was incubated with the labeled double-stranded probe (~50,000 cpm) in the presence of 5 µg of nonspecific blocker, poly(dI-dC) in binding buffer (10 mM Tris-HCl, pH 7.5, 100 mM

NaCl, 1 mM EDTA, 0.2% Nonidet P-40, and 0.5 mM DTT) at 25°C for 20 min. Specific competition was performed by adding 100 ng of unlabeled double-stranded ICAM-1 olignucleotide to the nuclear extract from the sample with the greatest nuclear binding (i.e. t=2 hours), while for nonspecific competition,100 ng of unlabeled double-stranded mutant ICAM-1 olignucleotide (5'-TAGCTTCTAGATTAGGGAGCTGAAG-3') that does not bind

NF-κB, was added. The mixture was separated by electrophoresis on a 5% polyacrylamide gel in 1 x Tris glycine EDTA buffer (20). Gels were vacuum dried and subjected to autoradiography and phosphoimager analysis.

Western Analysis. Liver tissue homogenate samples were separated on a 15% SDS-PAGE under nonreducing condition (21). Equivalent loading of the gel was determined by quantitation of protein as well as by Coomassie staining of the gel. Separated proteins were electroblotted onto PVDF membrane and blocked for 1 h at room temperature with Tris-buffered saline containing 1% BSA. The membranes were then incubated with a 1:1000 dilution of mouse anti-rat ICAM-1 antibody (Serotec Ltd. Oxford, England) at room temperature for 1 h. Antigen-antibody complexes were identified with goat anti-mouse IgG tagged with horseradish peroxidase (Sigma, St. Louis, MO) and exposed to the enhanced chemiluminesence detection system (Amersham, Arlington Heights, IL) according to the manufacturer's instructions.

Statistical Analysis. Results are expressed as mean ± SEM of the indicated number of experiments. Statistical significance among group means was assessed by Analysis of Variance. Student Neuman-Keuls post-hoc testing was performed.

RESULTS:

Glutathione depletion by DEM: As a measure of the ability of DEM to induce thiol oxidation in the liver, the effect of DEM on reduced glutathione, the major intracellular non-protein thiol, was shown (Figure 1). At both concentrations tested, DEM caused a rapid and profound lowering of GSH in liver tissue. Recovery occurred in a dose dependent fashion but levels were still ~30% reduced by 7 hours. DEM at 3 mmol/kg was used in the majority of studies reported except for the dose response studies.

Effect of DEM on hepatocellular enzyme release: As demonstrated in Figure 2A, LPS/GalN induced an increase in serum AST levels by 6 hours after LPS treatment. Intraperitoneal injection of DEM 30 minutes prior to LPS resulted in a dose dependent decrease in enzyme release, while DEM alone (3 mmol/kg) had no effect. To show the effect of DEM over the 6 hour experimental period, a time course of its effect was performed (Figure 2B). DEM was shown to inhibit AST elevation in LPS/GalN animals over the entire duration of the experimental period. To show the optimal timing of DEM administration, this agent was administered at varying time points relative to LPS/GalN. Figure 2C illustrates that treatment up to one hour before LPS/GalN prevented enzyme release, while delayed administration was ineffective.

Another glutathione depleting agent, phorone, was evaluated to determine its effect on LPS/GalN-induced liver injury. As shown in Figure 2D, pretreatment with phorone similarly caused a significant reduction in AST release in LPS/GalN animals compared to untreated animals. These findings suggest an effect related to thiol manipulation rather than a nonspecific effect of the agent. BSO and other glutathione depleting agents would also be useful.

Histological Evaluation of the effect of DEM on liver inflammation. To gain insight into the mechanism of the protective effect of DEM, liver sections were evaluated by light microscopy (Figure 3). Compared to sham-treated livers (left panel), livers from LPS/GalN-treated animals showed edematous hepatocytes and a loss of the normal architecture. There were areas of focal necrosis with a prominent neutrophil infiltration in the parenchyma (arrow). Finally, multiple apoptotic hepatocytes were observed (arrowhead). Treatment with DEM markedly attenuated the changes observed in LPS/GalN animals. Normal architecture was largely restored and the PMN infiltrate was diminished. Apoptotic hepatocytes were rarely observed.

Quantitative analysis of parenchymal infiltration by PMNs observed using light microscopy revealed that the increase induced by LPS/GalN was markedly reduced by DEM pretreatment (Table 1). Total MPO activity was also used to evaluate whole organ sequestration of PMNs. Similar to that observed for the parenchymal neutrophil count, there was an inhibition of the MPO activity in LPS/GalN animals following DEM treatment compared to LPS/GalN alone (Table 1).

Apoptosis in hepatocytes was more clearly delineated using an in situ end labeling assay. A representative experiment is shown in Figure 4. Consistent with the morphological changes seen in Figure 3, these studies confirmed that the LPS/GalN-induced increase in apoptosis was attenuated in animals pretreated with DEM. These changes are quantitated in Table 2.

Effect of DEM on endothelial cell adhesion molecule expression: Previous studies have shown that upregulation of ICAM-1 and VCAM-1 in the liver following LPS/GalN contribute to the parenchymal accumulation of PMNs and the development of hepatocellular necrosis (3,4). Figure 5 shows the effect of DEM on the levels of mRNA for each of these genes at various time points after LPS/GalN. LPS/GalN

caused a marked increase in ICAM-1 mRNA by 2 hours, peaking at 4 hours and beginning to diminish by 6 hours. A similar pattern was observed for VCAM-1. DEM totally prevented these changes. The housekeeping gene G3PDH showed comparable loading of mRNA in each lane.

To show the effect of DEM on ICAM-1 protein levels in the liver, Western blot analysis was performed. As shown in Figure 6, DEM prevented the LPS/GalN-induced rise in total liver ICAM-1 protein, without itself having an effect.

Effect of DEM on NF-κB translocation in liver. The effect of DEM on liver ICAM-1 expression was shown in further detail. The NF-κB binding region in the promoter of the ICAM-1 gene has been shown to be important in the initiation of gene transcription (19). To show how DEM influences binding of NF-κB to the ICAM-1 promoter, gel shift assays were performed on liver using the consensus binding sequence specific for ICAM-1. Figure 7 shows that LPS/GalN induces a marked and rapid increase in NF-κB binding with subsequent diminution over the experimental period. Pretreatment with DEM obviated this increase. The specificity of the binding was demonstrated by the ability of excess cold probe to compete for binding, while the mutant probe failed to do so.

Effect of DEM on Circulating PMN CD11b/CD18 expression. β2 integrins on neutrophils have also been shown to contribute to neutrophil transmigration into the hepatic parenchyma and the development of hepatocellular necrosis (5). We therefore investigated how DEM alters the LPS/GalN -induced upregulation of CD11b on circulating PMNs (Figure 8). CD11b expression on circulating PMNs was studied at t=3.5 hours after LPS/GalN administration. LPS/GalN caused an ~3-fold increase in CD11b compared to control ($p < 0.05$). In animals simultaneously receiving DEM,

CD11b was partially reduced, although this did not achieve statistical significance. Further, the magnitude of the reduction was relatively small compared to the inhibition of neutrophil infiltration in the liver seen with DEM treatment. These data show that the effect on circulating neutrophils was a minor contributor to the protection exerted by DEM.

Role of altered TNF in ICAM-1 expression and apoptosis. Studies using endotoxin-resistant mice have suggested that TNF plays a major role in LPS-induced upregulation of ICAM-1 in the liver as well as in the induction of apoptosis (3). To determine whether DEM might be exerting its effect in part through altering TNF, levels of TNF mRNA were evaluated in LPS/GalN animals treated with and without DEM. As shown in Figure 9, DEM prevented the LPS-induced rise in TNF mRNA in the liver. DEM also inhibited the LPS/GalN rise in serum TNF levels (data not shown). Considered together, these findings show that the beneficial effect of DEM on liver injury and apoptosis is due to a diminution in TNF release. We therefore performed studies to show that DEM directly protects the liver from the effects of TNF on hepatocellular necrosis and apoptosis. Intraperitoneal TNF injection (15 μg/kg) plus GalN caused a significant increase in serum AST levels at 6 hours (Figure 10). This increase was significantly attenuated in animals pretreated with DEM. In addition, the ability of TNF to cause hepatocyte apoptosis as assessed by morphological criteria as well as by in situ end labeling was markedly inhibited when TNF injection was preceded by administration of DEM (Table 3).

DISCUSSION:

The present studies demonstrate that agents characterized by their ability to cause thiol oxidation are able to prevent hepatocellular necrosis and apoptosis in a

rodent endotoxemia model. The findings that DEM exerted this protection following administration of a distinct inflammatory stimulus (i.e. TNF) and also without markedly affecting LPS-induced upregulation of PMN CD11b suggests that the effect is not simply due to chelation of endotoxin or inhibition of its binding in the liver. This is supported by *in vitro* studies where DEM had no effect on LPS-induced upregulation of neutrophil CD11b (data not shown). Rather, the data suggest that DEM has antiinflammmatory effects in the liver that preclude injury. Specifically, DEM was shown to prevent upregulation of two endothelial adhesion molecules, ICAM-1 and VCAM-1, which are known to be integral to neutrophil transmigration into the liver parenchyma and subsequent initiation of hepatocellular necrosis. DEM also inhibited the induction of hepatocyte apoptosis, in response to both endotoxin and TNF. Considered together, these findings show that this group of pharmacological agents exerts beneficial effects in the prevention of various liver diseases whose pathogenesis is related to neutrophil infiltration and/or apoptosis.

The inhibition of LPS-induced upregulation of ICAM-1 and VCAM-1 as well as TNF may be related to the ability of DEM to alter signaling pathways in endothelial cells and Kupffer cells respectively. Specifically, in animals treated with LPS/GalN, DEM prevented the nuclear translocation of NF-κB as assessed by electrophoretic mobility shift assays using the ICAM-1 specific consensus binding sequence. Ledebur and Parks previously demonstrated that the κB binding site is the most important transcriptional regulatory element in the ICAM-1 promoter (19), suggesting a causal relationship between reduced NF-κB translocation in the liver and impaired upregulation of ICAM-1 in LPS/GalN animals. The redox state of the cell has been shown to modulate various aspects of cell signaling relevant to the findings observed in the present studies. For

example, glutathione depletion using diamide was recently reported to inhibit ubiquitin-conjugating activity and ubiquitin-dependent proteolysis (22). Since IκB degradation is primarily mediated by this pathway (23), its persistence may have contributed to impaired NF-κB translocation. In this regard, we have recently reported that DEM causes delayed degradation of IκB in LPS-treated human umbilical vein endothelial cells (24). Alternatively, since NF-κB reduction by thioredoxin is required for NF-κB DNA binding, thiol oxidation may regulate NF- B dependent gene activation at the nuclear level by preventing the binding of NF- B to its DNA binding site (25). We investigate the mechanisms most responsible for impaired NF-κB translocation and reduced ICAM-1 expression in endothelial cells.

Inhibition of either ICAM-1 or VCAM-1 endothelial cell adhesion molecules or neutrophil β_2 integrins using specific antibodies has been shown to prevent hepatocellular necrosis without altering the total whole organ accumulation of these cells (3-5, 26). Histological studies of the liver specimens revealed that PMNs remained sequestered in the sinusoids rather than transmigrated into the parenchyma, where they might exert hepatocyte injury. Based on these studies, it has been postulated that neutrophil β integrin- endothelial cell interaction contribute mainly to the neutrophil transmigration and not to their initial sequestration in the liver. In the present studies, DEM treatment caused a reduction in both parenchymal infiltration and in total liver neutrophil sequestration, as measured by total liver MPO activity and histology. Several possibilities may account for the discrepancy between the prior reports and our findings. First, DEM exerts a broader inhibition of endothelial cell adhesion molecules than the antibody studies. Specifically, this agent inhibited upregulation of both ICAM-1 and VCAM-1 by LPS/GalN, while in the inhibitor studies, the activity of either ICAM-1 or

VCAM-1 was prevented. Whether DEM blocked other important endothelial adhesion molecules, such as E-selectin, as part of a broad effect on endothelial cell activation remains to be determined. Second, DEM may have affected the generation of various inflammatory mediators that contribute to the sinusoidal accumulation of PMNs. Jaeschke *et al* reported that TNF and complement factors generated in the early phase of endotoxemia contribute to neutrophil sequestration (5). In the present studies, TNF mRNA expression and TNF release was reduced in DEM-treated animals. Inhibition of the TNF-induced actin polymerization may have prevented the increase in neutrophil stiffness considered responsible for sequestration of cells in the sinusoidal vasculature (27,28). Considered together, these possibilities may explain the finding of both reduced hepatocellular necrosis and neutrophil sequestration following treatment with DEM.

DEM was shown to prevent the LPS/GalN-induced increase in hepatocyte apoptosis. This effect was, at least in part, attributable to the ability of DEM to inhibit TNF production. However, in studies using TNF as the inflammatory stimulus, DEM caused similar protection against the initiation of apoptosis, suggesting a direct effect of thiol oxidation on the pathways leading to apoptosis in hepatocytes. In this regard, Kim and colleagues recently reported that induction of heat shock protein 70 through GSH oxidation by S-nitroso-N-acetylpenicillamine (SNAP) protected cultured rat hepatocytes from TNFα-induced apoptosis (29). The time course of hsp70 induction by SNAP was too slow to account for the protection observed in the present studies. However, this does not rule out the possibility that other stress proteins might have been protective. Recent studies by Jaeschke *et al* have reported that activation of caspase-3-like proteases in hepatic parenchymal cells following TNF-α administration is essential for the induction of apoptosis (7). Direct or indirect modulation of this protein by glutathione

depletion may have contributed to the anti-apoptotic effect of DEM. Nobel and colleagues have reported that thiol-oxidizing agents may inhibit apoptosis by preventing the proteolytic activation of caspase-3 (30). Further studies are warranted to discern whether thiol oxidation *in vivo* may have acted by altering caspase-3 activation.

The findings presented in this manuscript appear somewhat at variance with previous reports demonstrating the ability of antioxidant-type agents to prevent LPS-stimulated upregulation of ICAM-1 and TNF in the liver and also lessen liver injury (31-33). Neuschwander-Tetri and colleagues suggested that the effect was mediated through redox manipulation rather than through changes in glutathione levels per se, since pharmacological intervention preventing the N-acetyl-cysteine-induced rise in reduced glutathione did not preclude the ability of this agent to inhibit LPS-induced Kupffer cell TNF release (33). We therefore show that thiol-oxidizing agents and glutathione depleting agents such as DEM may represent novel alternatives for redox manipulation which appear to exert potent antiinflammatory effects through altering intracellular signalling pathways leading to proinflammatory gene expression. In the present studies, they reduced hepatocellular necrosis and apoptosis in the rodent LPS/D-galactosamine model. Their potential use in other inflammatory states characterized by PMN-endothelial cell interaction and/or apoptosis is tested.

Table 1: Effect of DEM on neutrophil infiltration in the liver

	Parenchymal PMNs (percent of hepatocytes counted)[a]	Myeloperoxidase (Δ O.D./minute/mg protein)[b]
Control	0.3	0.85±0.42
DEM alone (3mmol/kg)	ND[c]	0.81±0.09
LPS/GalN	15.3	24.79±11.10
LPS/GalN plus DEM (3mmol/kg)	5.3	1.08±0.12*

a: Number of neutrophils within the parenchyma expressed as a percentage of the number of hepatocytes counted. Multiple fields were counted comprising at least 700 parenchymal cell in each group.

b: The data represent the mean and standard error of the mean for 2-3 animals in each group. * $p<0.05$ versus LPS/GalN

c: ND: not determined

Table 2: Effect of DEM on apoptosis in the liver following LPS/GalN

	Morphology[a]	In situ end labeling[b]
Control	0.1%	0
DEM alone (3mmol/kg)	0.1%	ND[c]
LPS/GalN	6.2%	2.1%
LPS/GalN plus DEM (3mmol/kg)	0.5%	0

a: Data represent the percentage of cells with morphological changes of apoptosis. For each group, a minimum of 500 cells in multiple fields was counted.

b: Data represent the percentage of cells with apoptosis based on in situ end labeling. For each group, a minimum of 700 cells in multiple fields was counted.

c: ND: not determined

Table 3: Effect of DEM on apoptosis in the liver following TNF/GalN

	Morphology[a]	In situ end labeling[b]
Control	0.1%	0
DEM alone (3mmol/kg)	0.1%	0.2%
LPS/GalN	8.5%	1.9%
LPS/GalN plus DEM (3mmol/kg)	0.8%	0.2%

a: Data represent the percentage of cells with morphological changes of apoptosis. For each group, a minimum of 500 cells in multiple fields was counted.

b: Data represent the percentage of cells with apoptosis based on in situ end labeling. For each group, a minimum of 525 cells in multiple fields was counted.

FIGURE LEGENDS:

Figure 1: The effect of DEM on reduced glutathione levels in the liver. The data represent the mean and SEM of three independent studies. * $p<0.05$ versus t=0 for each group.

Figure 2:

A: The effect of DEM on serum AST levels. Animals were injected with varying doses of DEM at 30 minutes prior to LPS/GalN ip and sacrificed at t=6 hours after LPS/GalN for determination of serum AST levels. The data represent the mean and SEM of at least 7 animals per group. ** $p< 0.05$ versus control; * $p< 0.05$ versus LPS/GalN.

B: Time course of the effect of DEM on serum AST levels. Animals were injected with Saline or LPS/GalN with or without DEM (3mmol/kg) and blood was drawn via an arterial line at the indicated time point for measurement of serum AST level. The data represent the mean and SEM of 3 animals per group at each time point. * $p< 0.05$ versus other groups at same time point

C: Delayed DEM administration and AST release. DEM (3 mmol/kg) was administered at various times relative to LPS/GalN injection and evaluated for serum AST levels at t=6 hours after LPS/GalN. The data represent the mean and SEM of 3 animals in each group. * $p<0.05$ versus LPS/GalN

D: The effect of phorone on LPS\GalN induced AST release. Animals were injected with phorone (250 mg/kg) 30 min prior to LPS\GalN and sacrificed at t=6 hours for evaluation of serum AST levels. The data represent the mean and SEM of three animals per group. * $p< 0.05$ versus Controls **$p<0.05$ versus LPS/GalN

Figure 3: Histological evaluation of liver morphology following DEM treatment. Animals were injected with LPS/GalN or saline with or without pretreatment with DEM. Animals were sacrificed at t=6 hours and livers were processed for evaluation by light microscopy as described in the METHODS. The data are representative of two separate studies for each group. DEM alone did not differ from sham. In the middle panel, the arrowhead indicates an infiltrating neutrophil and the Arrow denotes an apoptotic cell. Magnification 400X

Figure 4: Determination of apoptosis by in situ end labeling Animals were injected with LPS/GalN or saline with or without pretreatment with DEM. Animals were sacrificed at t=6 hours and livers were processed for in situ end labeling as described in the METHODS. The data are representative of two separate studies for each group. Magnification 400X

Figure 5: ICAM-1 and VCAM-1 mRNA expression following DEM treatment: Animals were treated with DEM (3 mmol/kg) at 30 min prior to LPS/GalN and sacrificed 2,4 and 6 hours later. Liver samples were processed for Northern blot analysis as described in the METHODS using the cDNA probe for ICAM-1 (Panel A) and VCAM-1 (Panel B). For each of ICAM-1 and VCAM-1, the data in the left panel are representative of 3 independent studies performed at each time point. Corresponding G3PDH mRNA is shown as evidence of comparable loading between lanes. Mean densitometry for ICAM-1 (Panel A, right side) and VCAM-1 (Panel B, right side) for the three studies is shown following correction for G3PDH mRNA loading. *$p<0.05$ versus similar time point for LPS/GalN plus DEM

Figure 6: ICAM-1 protein following DEM treatment: Animals were treated with DEM (3 mmol/kg) or vehicle at 30 min prior to LPS/GalN and sacrificed 4 and 6 hours later. Liver samples were processed for Western blot analysis as described in the METHODS. The data are representative of 3 independent studies performed at each time point.

Figure 7: NF-κB translocation in liver following LPS/GalN treatment: Representative autoradiograph of EMSA showing time course of LPS/GalN-induced NF-κB nuclear translocation in liver tissue. Liver tissue was obtained from LPS/GalN animals with or without DEM (3mmol/kg) at the times noted. The probe for EMSA was a ^{32}P-ATP-end labeled double-strand construct corresponding to a sequence in the ICAM-1 proximal promoter region containing the NF-κB motif. Cold competition and competition using a mutant probe are also shown for sample in lane 3. A representative of three independent experiments is shown.

Figure 8: Effect of DEM on CD11b expression on circulating PMNs: Rats were treated with LPS/GalN with or without pretreatment with DEM (3 mmol/kg). At t=3.5 hours, blood was withdrawn by retroorbital puncture into heparinized syringes for evaluation of whole blood CD11b expresssion by flow cytometry as described in the MATERIAL AND METHODS section. The data are expressed as percent of control and represent the mean and SEM of 3 studies per group. * $p<0.05$ versus control.

Figure 9: TNF mRNA expression following DEM treatment: Animals were treated with DEM (3 mmol/kg) at 30 min prior to LPS/GalN and sacrificed 2,4 and 6 hours later. Liver samples were processed for Northern blot analysis and probed with the cDNA for

murine TNF-α as described in the MATERIALS AND METHODS section. The data are representative of 3 independent studies performed at each time point. Corresponding G3PDH mRNA is shown as evidence of comparable loading between lanes. Mean densitometry for TNF-α mRNA for the three studies is shown following correction for G3PDH mRNA loading. *p<0.05 versus similar time point for LPS/GalN plus DEM

Figure 10: The effect of DEM on serum AST levels following TNF/GalN induced liver injury: Animals were injected with DEM (3 mmol/kg) at 30 minutes prior to TNF/GalN ip and sacrificed at t=6 hours after TNF/GalN for determination of serum AST levels. The data represent the mean and SEM of at least 4 animals per group. * p< 0.05 versus control; ** p< 0.05 versus TNF/GalN.

The compounds of this invention are preferably incorporated into pharmaceutical dosage forms suitable for the desired administration route such as tablets, dragees, capsules, granules, suppositories, solutions, suspensions and lyophilized compositions to be diluted to obtain injectable liquids. The dosage forms are prepared by conventional techniques and in addition to the compounds of this invention could contain solid or liquid inert diluents and carriers and pharmaceutically useful additives such as liposomes, aggregants, disaggregants, salts for regulating the osmotic pressure, buffers, sweeteners and colouring agents. Slow release pharmaceutical forms for oral use may be prepared according to conventional techniques.

Pharmaceutical compositions used to treat patients having diseases, disorders or abnormal physical states could include SAG-A or another peptide of the invention and an acceptable vehicle or excipient (Remington's Pharmaceutical Sciences 18th ed, (1990, Mack Publishing Company) and subsequent editions). Vehicles include saline and D5W (5% dextrose and water). Excipients include additives such as a buffer, solubilizer, suspending agent, emulsifying agent, viscosity controlling agent, flavor, lactose filler, antioxidant, preservative or dye. There are preferred excipients for stabilizing peptides for parenteral and other administration. The excipients include serum albumin, glutamic or aspartic acid, phospholipids and fatty acids. The protein may be formulated in solid or semisolid form, for example pills, tablets, creams, ointments, powders, emulsions, gelatin capsules, capsules, suppositories, gels or membranes. Routes of administration include oral, topical, rectal, parenteral (injectable), local, inhalant and epidural administration. The compositions of the invention may also be conjugated to transport molecules to facilitate transport of the molecules. The methods for the preparation of pharmaceutically acceptable compositions which can be administered to patients are known in the art.

The pharmaceutical compositions can be administered to humans or animals. Dosages to be administered depend on individual patient condition, indication of the drug, physical and chemical stability of the drug, toxicity, the desired effect and on the chosen route of administration (Robert Rakel, ed., Conn's Current Therapy (1995, W.B.

Saunders Company, USA)). The pharmaceutical compositions are used to treat diseases caused by streptococcal infections such as endocarditis, cellulitis, brain abscesses, glomerulonephritis, impetigo, meningitis, necrotizzing, osteomyelitis, pharyngitis, rheumatic fever, pneumonia, AIDS, rheumatic carditis, rheumatic fever and toxic shock.

Suitable mimetics and their preparation would be readily apparent to one skilled in the art. For example, mimetics and their preparation are disclosed in US Patent Nos. 5,139,807, 5,124,166, 5,108,568, 5,093,142, 5,091,396, 5,068,233.

The present invention has been described in detail and with particular reference to the preferred embodiments; however, it will be understood by one having ordinary skill in the art that changes can be made thereto without departing from the spirit and scope thereof.

All publications, patents and patent applications are herein incorporated by reference in their entirety to the same extent as if each individual publication, patent or patent application was specifically and individually indicated to be incorporated by reference in its entirety. In particular, U.S. Patent Application No. 08/796,292 (Title: Anti-inflammatory & Anti-Pyretic Method; Filing Date: February 7, 1997) and Canadian application no. 2,197,058 (Title: Anti-inflammatory Agent; Filing Date: February 7, 1997) are incorporated by reference in their entirety.

REFERENCES

1. Jaeschke H, Smith CW. Mechanisms of neutrophil-induced parenchymal cell injury. [Review] J Leukocyte Biol 1997; 61:647-653.

2. Jaeschke H, Smith CW. Cell adhesion and migration III. Leukocyte adhesion and transmigration in the liver vasculature. Am J Physiol Gastrointest Liver Physiol 1997; 273:G1169-G1173.

3. Essani NA, Fisher MA, Farhood A, Manning AM, Smith CW, Jaeschke H. Cytokine-induced upregulation of hepatic intercellular adhesion molecule-1 messenger RNA expression and its role in the pathophysiology of murine endotoxin shock and acute liver failure. Hepatology 1995; 21:1632-1639.

4. Essani NA, Bajt ML, Farhood A, Vonderfecht SL, Jaeschke H. Transcriptional activation of vascular cell adhesion molecule-1 gene in vivo and its role in the pathophysiology of neutrophil-induced liver injury in murine endotoxin shock. Journal of Immunology 1997; 158:5941-5948.

5. Jaeschke H. Chemokines and liver inflammation: the battle between pro- and anti-inflammatory mediators. Hepatology 1997; 25:252-253.

6. Volpes R, Van den Oord JJ, Desmet VJ. Immunohistochemical study of adhesion molecules in liver inflammation. Hepatology 1990; 12:59-65. ICAM.

7. Jaeschke H, Fisher MA, Lawson JA, Simmons CA, Farhood A, Jones DA. Activation of caspase 3 (CPP32)-like proteases is essential for TNF-alpha-induced hepatic parenchymal cell apoptosis and neutrophil-mediated necrosis in a murine endotoxin shock model. Journal of Immunol 1998; 160:3480-3486.

8. Brisseau GF, Dackiw AP, Cheung PY, Christie N, Rotstein OD. Posttranscriptional regulation of macrophage tissue factor expression by antioxidants. Blood 1995; 85:1025-1035.

9. Hwang C, Sinskey AJ, Lodish HF. Oxidized redox state of glutathione in the endoplasmic reticulum. Science 1992; 257:1496-1502.

10. Meyer M, Schreck R, Baeuerle PA. H_2O_2 and antioxidants have opposite effects on activation of NF-kappaB and AP-1 in intact cells: AP-1 as secondary antioxidant-responsive factor. EMBO J 1993; 12:2005-2015.

11. Fialkow L, Chan CK, Rotin D, Grinstein S. Activation of mitogen-activated protein kinase signaling pathways in neutrophils: role of oxidants. J Biol Chem 1994; 269:31234

12. Nathens AB, Bitar R, Watson RWG, Issekutz TB, Marshall JC, Dackiw APB, et al. Thiol-mediated regulation of ICAM-1 expression in endotoxin-induced acute lung injury. J Immunol 1998; 160:2959-2966.

13. Wijsman JH, et al. A new method to detect apoptosis in paraffin sections: In situ end-labeling of fragmented DNA. Journal of Histochemistry and Cytochemistry 1993; 41:7-12.

14. Davreux CJ, Soric I, Nathens AB, Watson RW, McGilvray ID, Suntres ZES, PN, et al. N-acetyl cysteine attenuates acute lung injury in the rat. Shock 1997; 8:432-438.

15. Jocelyn PC. Spectrophotometric assay of thiols. Methods Enzymol 1987; 143:44-67.

16. Allen RC. Phagocytic leukocyte oxygenation activities and chemiluminescence: a kinetic approach to analysis. Meth Enzymol 1986; 133:449-493.

17. Chomczynski P, Sacchi N. Single-step method of RNA isolation by acid guanidinium thiocyanate-phenol-chloroform extraction. Analytical Biochemistry 1987; 162:156-159.

18. Deryckere F, Gannon F. A one-hour minipreparation technique for extraction of DNA-binding proteins from animal tissues. Biotechniques 1994; 16:405

19. Ledebur HC, Parks TP. Transcriptional regulation of the intercellular adhesion molecule-1 gene by inflammatory cytokines in human endothelial cells. Essential roles of a variant NF-kB site and p65 homodimers. J Biol Chem 1995; 270:933-943.

20. Garner MM, Revzin A. A gel electrophoresis method for quantifying the binding of proteins to specific DNA regions: applications to components of *Escherichia coli* lactose regulatory system. Nucleic Acids Res 1981; 9:3047-3060.

21. Burnette WH. Western blotting: Electrophoretic transfer of proteins from SDS-polyacrylamide gels to unmodified nitrocellulose and radiographic detection with antibody and radioiodinated protein A. Anal Biochem 1981; 112:195-203.

22. Obin M, Shang F, Gong X, Handelman G, Blumberg J, Taylor A. Redox regulation of ubiquitin-conjugating enzymes: mechanistic insights using the thiol-specific oxidant diamide. FASEB J 1998; 12:561-569.

23. Chen Z, Hagler J, Palombella VJ, Melandri F, Scherer D, Ballard D, et al. Signal-induced site-specific phosphorylation targets I kappa B alpha to the ubiquitin-proteosome pathway.. Genes and Development 1995; 9:1586-1597. nf-kb.

24. Jones JJ, Bitar R, Rotstein OD. Glutathione depletion inhibits IκB-α degradation in human umbilical vein endothelial cells. [Abstract] Presented at the Annual Surgical Infection Society Meeting, New York City, NY, May 1998, p19.

25. Hayashi T, Ueno Y, Okamoto T. Oxidoreductive regulation of nuclear factor kappa B. Involvement of a cellular reducing catalyst thioredoxin. J Biol Chem 1993; 268:11380-11388.

26. Vollmar B, Senkel A, Menger MD. In vivo evidence that intercellular adhesion molecule-1 does not mediate endotoxin-induced hepatic leukocyte-endothelial interaction. J Hepatol 1995; 23:613-616.

27. Elbim C, Lefebvre M, Hakim J, Gougerot-Pocidalo MA. Effects of pentoxifylline on human polymorphonuclear neutrophil responses to TNF in whole blood. European Cytokine Network 1995; 6:113-120.

28. Erzurum SC, Downey GP, Doherty DE, Schwab B, 3d, Elson EL, Worthen GS. Mechanisms of lipopolysaccharide-induced neutrophil retention. Relative contributions of adhesive and cellular mechanical properties. Journal of Immunol 1992; 149:154-162.

29. Kim YM, de Vera ME, Watkins SC, Billiar TR. Nitric oxide protects cultured rat hepatocytes from tumor necrosis factor-alpha-induced apoptosis by inducing heat shock protein 70 expression. J Biol Chem 1997; 272:1402-1411.

30. Nobel CS, Burgess DH, Zhivotovsky B, Burkitt MJ, Orrenius S, SlaterAF. Mechanism of dithiocarbamate inhibition of apoptosis: thiol oxidation by dithiocarbamate disulfides directly inhibits processing of the caspase-3 proenzyme. Chemical Research in Toxicology 1997; 10:636-643.

31. Essani NA, Fisher MA, Jaeschke H. Inhibition of NF-kappa B activation by dimethyl sulfoxide correlates with suppression of TNF-alpha formation, reduced ICAM-1 gene transcription, and protection against endotoxin-induced liver injury [see comments]. Shock 1997; 7:90-96.

32. Sugino K, Dohi K, Yamada K, Kawasaki T. The role of lipid peroxidation in endotoxin-induced hepatic damage and the protective effects of antioxidants. Surgery 1998; 101:746-752. antioxidants.

33. Neuschwander-Tetri BA, Bellezzo JM, Britton RS, Bacon BR, Fox ES. Thiol regulation of endotoxin-induced release of tumour necrosis factor a from isolated rat Kupffer cells. Biochem J 1996; 320:1005-1010.

We claim

1. A method of decreasing cell apoptosis and/or cell necrosis in a mammal, comprising administering an effective amount of a glutathione depleting agent or a pharmaceutically acceptable salt thereof.

2. The method of claim 1, wherein the glutathione depleting agent is selected from the group consisting of diethylmaleate (DEM), a mimetic of DEM having glutathione depleting activity, phorone, a mimetic of phorone having glutathione depleting activity, buthionine sulfoximine (BSO), a mimetic of buthionine sulfoximine (BSO) having glutathione depleting activity and their equivalents.

3. The method of claim 1 or 2, wherein the cell is a hepatocyte, a leukocyte, an endothelial cell or an epithelial cell.

4. The method of any of claims 1 to 3, wherein cell apoptosis is caused by TNF or an apoptosis inducing agent.

5. The method of any of claims 1 to 4, wherein the cell apoptosis and/or cell necrosis occurs as a result of inflammation, neoplasis, or inherent pre-programmed cell death.

6. The method of any of claims 1 to 5, wherein the route of administration of the agent is selected from a group consisting of oral administration, aerosol administration, parenteral administration, cavity administration, rectal administration and air passage administration.

7. Use of a glutathione depleting agent or a pharmaceutically acceptable salt thereof in the manufacture of a medicament for decreasing cell apoptosis and/or cell necrosis.

8. Use of a glutathione depleting agent or a pharmaceutically acceptable salt thereof for decreasing cell apoptosis and/or cell necrosis.

9. The use of claim 7 or 8, wherein the glutathione depleting agent is selected from the group consisting of diethylmaleate (DEM), a mimetic of DEM having glutathione depleting activity, phorone, a mimetic of phorone having glutathione depleting activity, buthionine sulfoximine (BSO), a mimetic of buthionine sulfoximine (BSO) having glutathione depleting activity and their equivalents.

10. The use of any of claims 7 to 9, wherein the cell is a hepatocyte, a leukocyte, an endothelial cell or an epithelial cell.

11. The use of any of claims 7 to 10, wherein cell apoptosis is caused by TNF or an apoptosis inducing agent.

12. The use of any of claims 7 to 11, wherein the cell apotosis/or cell necrosis occurs as a result of inflammation, neoplasis, or inherent pre-programmed cell death.

13. The use of any of claims 7 to 12, wherein the route of administration of the agent is selected from a group consisting of oral administration, aerosol administration, parenteral administration, cavity administration, rectal administration, air passage administration.

14. A cell apoptosis and/or cell necrosis decreasing pharmaceutical composition, comprising a glutathione depleting agent or a pharmaceutically acceptable salt thereof, in association with a pharmaceutically acceptable carrier.

15. The composition of claim 14, wherein the glutathione depleting agent is selected from the group consisting of diethylmaleate (DEM), a mimetic of DEM having glutathione depleting activity, phorone, a mimetic of phorone having glutathione depleting activity, buthionine sulfoximine (BSO), a mimetic of buthionine sulfoximine (BSO) having glutathione depleting activity and their equivalents.

16. A pharmaceutical package, needle, kit or aerosol delivery device comprising the composition of claim 14 or 15.

17. A method of decreasing cell apoptosis and/or cell necrosis in a mammal, comprising administering an effective amount of the composition of claim 14 or 15.

18. Use of the composition of claim 14 or 15 in the manufacture of a medicament for decreasing cell apoptosis.

19. Use of the composition of claim 14 or 15 for decreasing cell apoptosis and/or cell necrosis.

20. The composition of claim 14 or 15 or the package, needle, kit or device of claim 16 for use in decreasing cell apoptosis and/or cell necrosis.

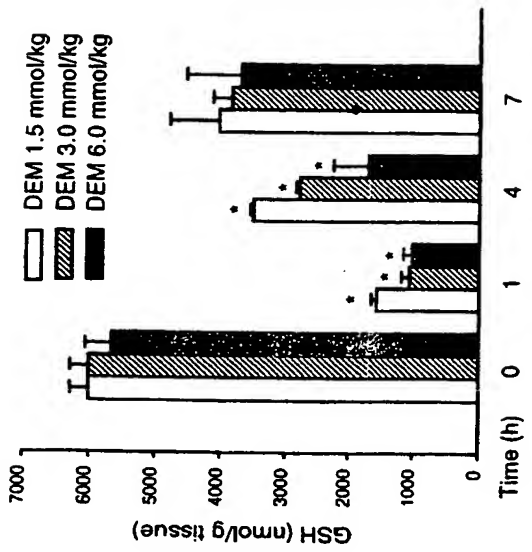
DEM 1.5 mmol/kg
DEM 3.0 mmol/kg
DEM 6.0 mmol/kg
GSH (nmol/g tissue)
7000
6000
5000
4000
3000
2000
1000
0
Time (h)
0
1
4
7

Figure 1

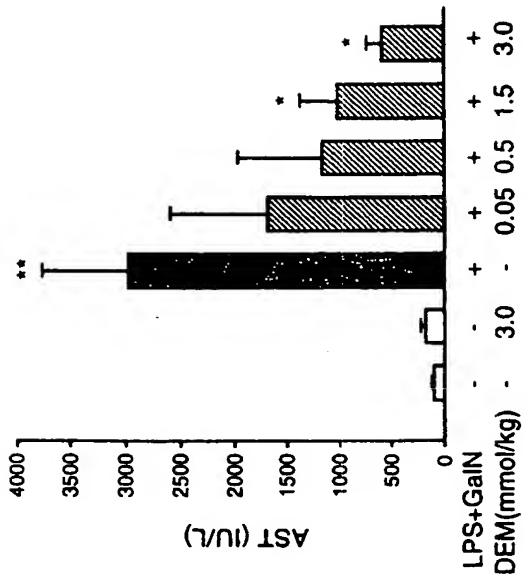
AST (IU/L)
4000
3500
3000
2500
2000
1500
1000
500
0
**
*
*
*
LPS+GalN - - + + + + +
DEM(mmol/kg) - 3.0 - 0.05 0.5 1.5 3.0

Figure 2A

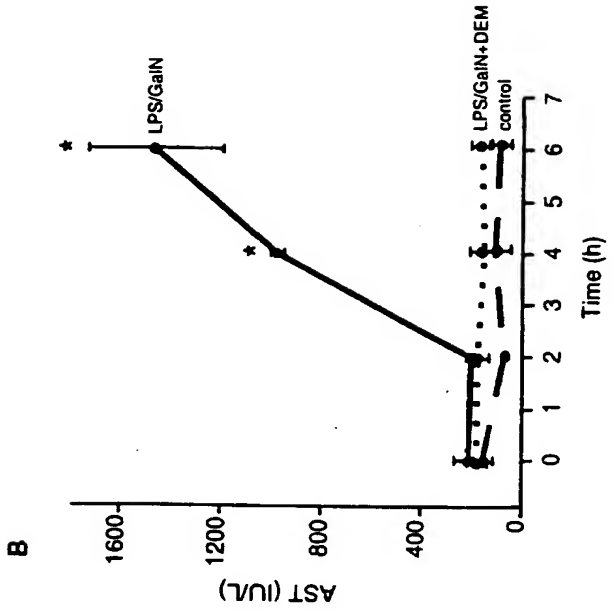
B
AST (IU/L)
1600
1200
800
400
0
0 1 2 3 4 5 6 7
Time (h)
LPS/GalN
LPS/GalN+DEM
control
*
*

Figure 2B

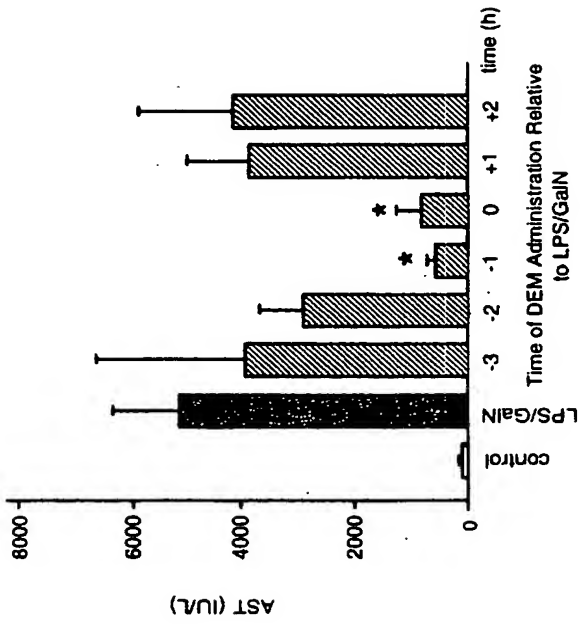
AST (IU/L)
8000
6000
4000
2000
0
control
LPS/GalN
-3
-2
-1
0
+1
+2
time (h)
Time of DEM Administration Relative to LPS/GalN
*
*

Figure 2C

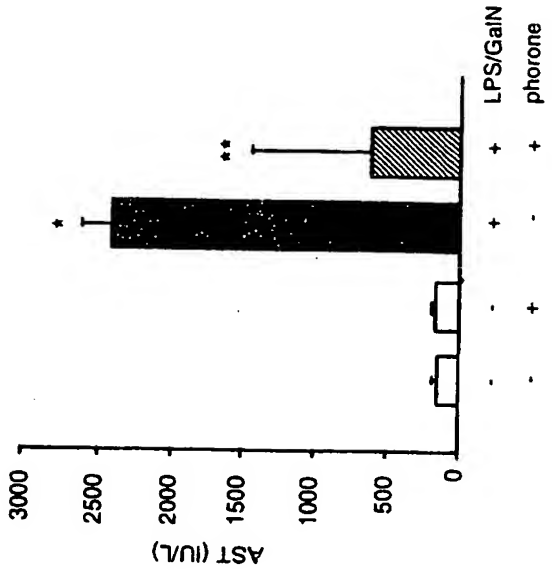

Figure 2D

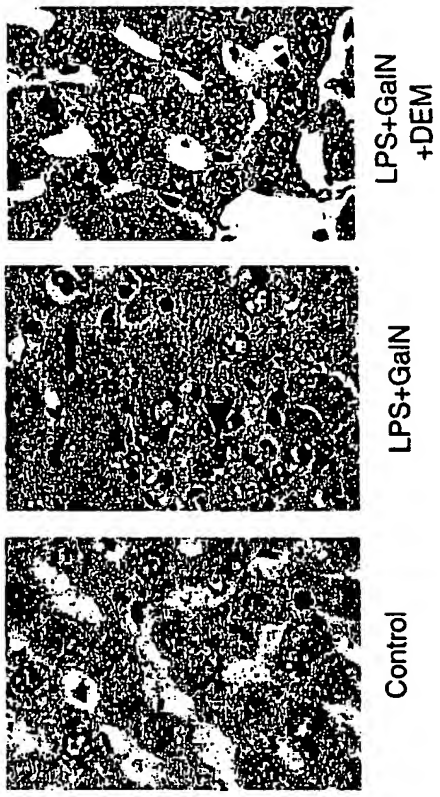

Figure 3

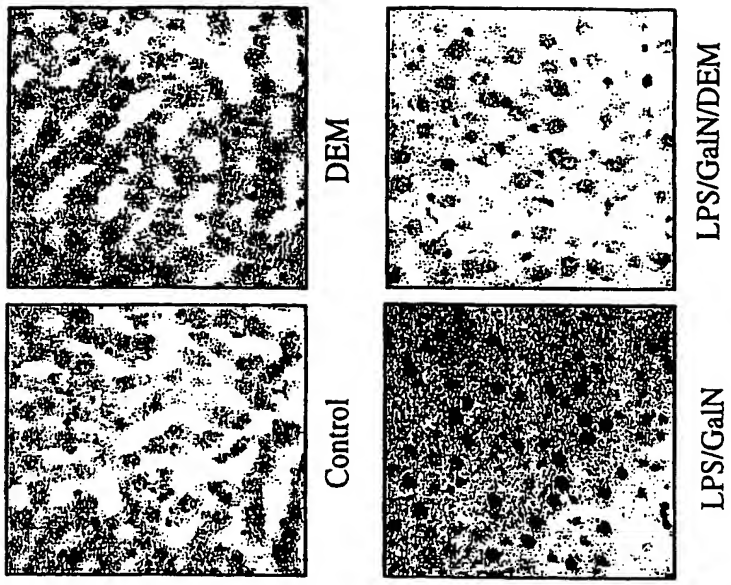

Figure 4

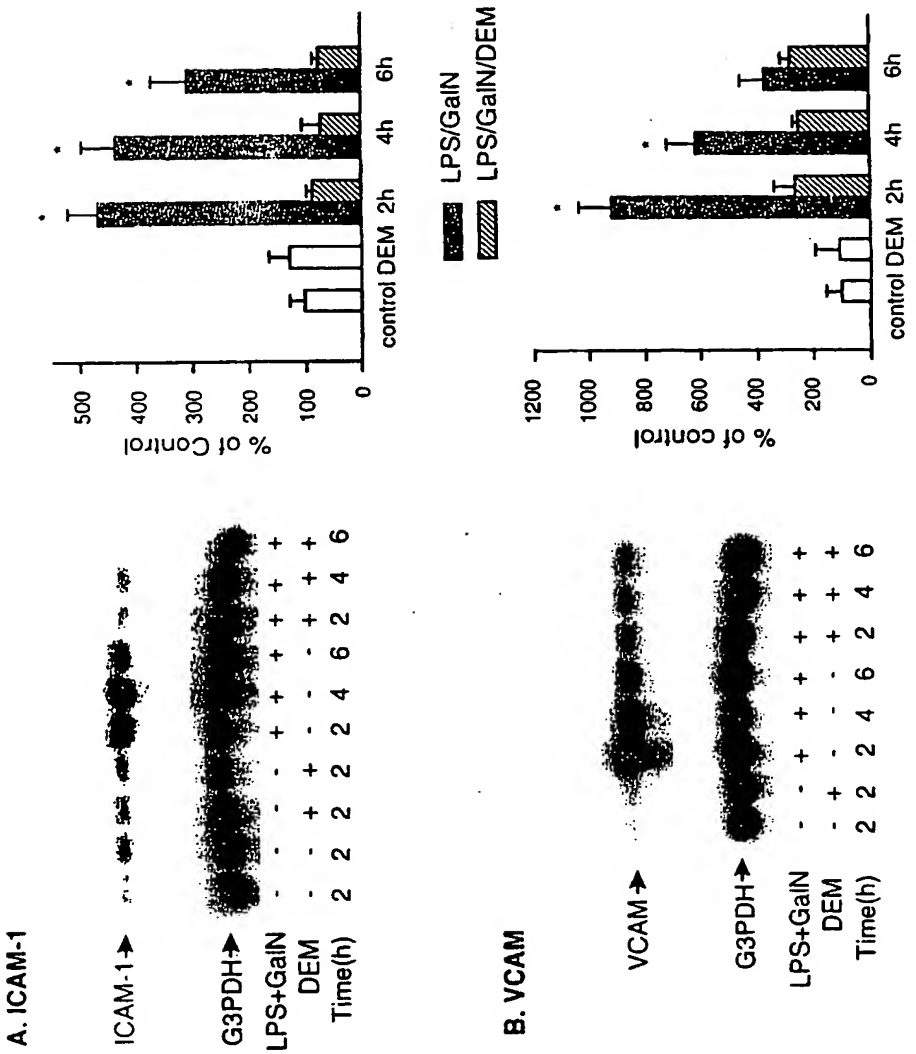
A. ICAM-1
ICAM-1
G3PDH
LPS+GalN - - - - + + - - + + + +
DEM - - + + - - + + - - + +
Time(h) 2 2 2 2 2 4 6 2 4 6
% of Control
500
400
300
200
100
0
control DEM 2h 4h 6h
LPS/GalN
LPS/GalN/DEM
B. VCAM
VCAM
G3PDH
LPS+GalN - - + + + + + + + + + +
DEM - + - - - + + + + + + +
Time(h) 2 2 2 4 6 2 4 6
% of control
1200
1000
800
600
400
200
0
control DEM 2h 4h 6h

Figure 5

Figure 6

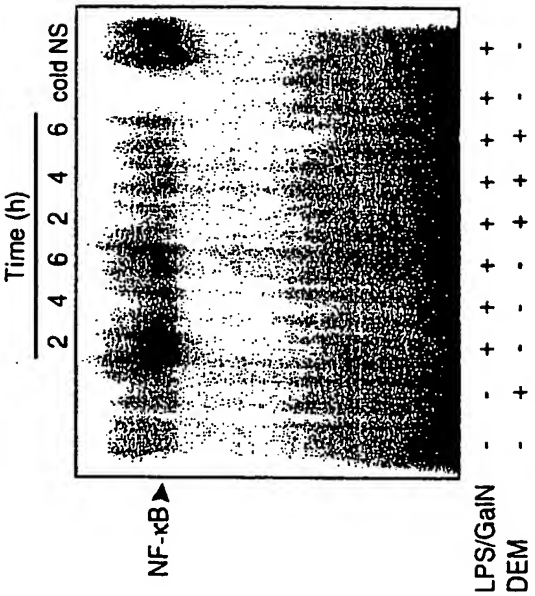

Figure #7

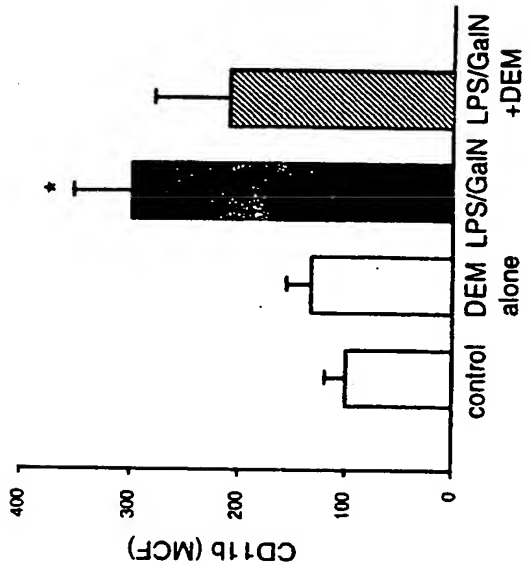
CD11b (MCF)
400
300
200
100
0
*
control
DEM alone
LPS/GalN
LPS/GalN +DEM

Figure #8

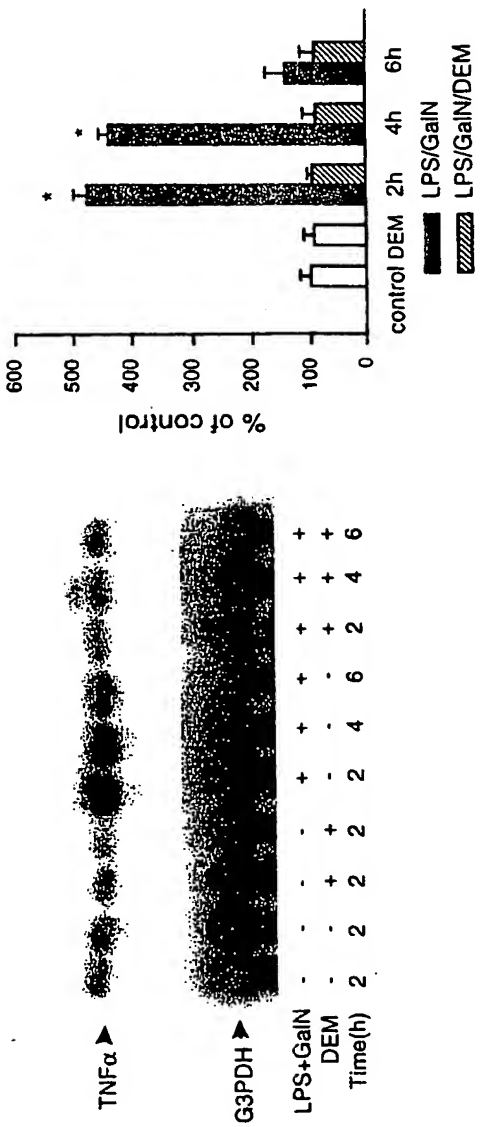
% of control
600
500
400
300
200
100
0
control DEM 2h 4h 6h
LPS/GalN
LPS/GalN/DEM
*
*
TNFα
G3PDH
LPS+GalN - - - + - + + + + +
DEM - - + + + + + + + +
Time(h) 2 2 2 2 2 4 6 2 4 6

Figure 9

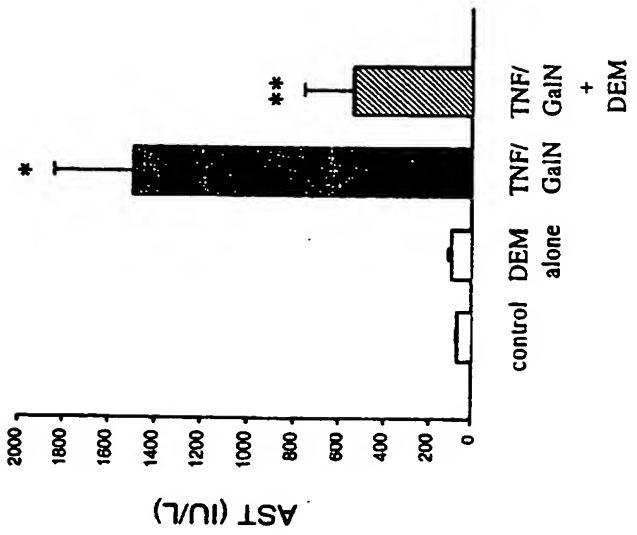
AST (IU/L)
2000
1800
1600
1400
1200
1000
800
600
400
200
0
*
**
control
DEM alone
TNF/ GalN
TNF/ GalN + DEM

Figure 10